Silicon (2023) 15:4473–4480
https://doi.org/10.1007/s12633-023-02352-3

ORIGINAL PAPER

Effect of Pressure on the Structure of SiO2 at the Glass Transition Temperature

Nguyen Thu Nhan[1] · **Nguyen Van Hong**[1] · **Mai Thi Lan**[1]

Received: 23 September 2022 / Accepted: 14 February 2023 / Published online: 28 February 2023

Abstract

The structural transformation of Silica system under compression at glass transition temperature (1475 K) investigated by molecular dynamics method. The structural features such as pair radial distribution function, coordination number, linkage and cluster distribution analyzed systematically. The tetrahedral coordination (SiO_4) maintained up to pressure of 5 GPa. Under compression, the structure tends to transit gradually from tetrahedral- to octahedral- coordination (SiO_6) via pentahedral ones (SiO_5). At pressure beyond 30 GPa, most of Si cation have octahedral coordination. The structural transitions at high-temperature models (1475 K) occurred at pressure higher than that at low temperature ones (500 K). In the 10–20 GPa range, the structure of model consisted of two large clusters of SiO_5 and SiO_6 revealing the structural homogeneity.

Keywords Molecular dynamics · Glass transition temperature · SiO_2 · Cluster · Links

1 Introduction

The relationship between the structure and physical properties of silica glass under pressure has always been of interest because of its wide application in all fields of science, technology, and life [1–5]. The glass transition temperature of silica is of particular interest because all glass products undergo this structural state transformation [6–8]. The essence of the structural phase transition is the breaking of bonds and the rearrangement of the atoms. Under the influence of temperature, the geometric structure such as distance and angle bonds in basic units is almost no changes. A slight change in volume corresponds to a change in the free volume region [9, 10]. At low temperature (500 K), under pressure up to 100 GPa, the structural change from tetrahedral to octahedral is quite abrupt in the pressure range of 10-20GPa [11]. Specifically, it shows a very rapid change in the ratio of the basic structural units SiO_4 to SiO_6. The structural change also reflected in the change in the short order and intermediate order range, the number of corner-, edge-, and face-shared links. That is a very rapid increase in the number of corner- and edge-shared bonds in the 15–20 GPa range. In report [12], when compressing amorphous SiO_2 at a pressure of 7.7 GPa and temperature of 600 K, there is a structural phase transition from the low-density phase to the high-density phase. This phase transition happens fast at temperatures below 600 K. At temperatures above 600 K, the density change is slow with increasing temperature. Reports in [13] also show the structural phase transition in glass SiO_2 from four-coordinated to six-coordinated structure in 15–50 GPa range. This phase transition is related to the increase of the Si–O pair bond distance. In report [14], the structural phase transition in liquid SiO_2 also occurs suddenly in the 10–20 GPa range. This change partly caused by the decrease of the O–O bond distances under compression. The work [15] also shows an important role of O in the process of structural change. Under compression, there is a change in the size and topology of SiO_x polyhedral. The ring structure also performed by simulation method at room temperature and at pressure up to17.5 GPa [16]. The report [17] shows that the higher the temperature, the more chemical bonds broken and hence the slower the structural phase transition, which will result in a qualitative change of the newly formed phase. The structural change predicted that, when the bonds broken, there will be relaxation of configurations and formation of clusters. However, understanding of structural phase transitions at high temperature, especially the glass transition temperature region has not been fully studied and many issues need to be elucidated.

✉ Nguyen Thu Nhan
nhan.nguyenthu@hust.edu.vn

[1] School of Engineering Physics, Hanoi University of Science and Technology, No. 1 Dai Co Viet, Hanoi, Vietnam

In this study, the structural phase transition process of SiO_2 structure under compression at the glass transition temperature of 1475 K investigated and clarified. The structural changes and their characteristics under pressure analyzed in detail. The visual method is also in this work to clarify the glassy network and structural heterogeneity.

2 Calculation Method

The models of amorphous SiO_2 containing 4998 atoms have been constructed by molecular dynamic (MD) at temperature 1475 K an in the 0–100 GPa range. Periodic boundary conditions and the van Beest-Kramer-van Santen (BKS) potential applied in this simulation. The detail about the simulation described in [18]. Initial configuration generated by randomly placing all atoms in a simulation box with density of 2.22 g/cm^3. Then the model heated up to 6000 K and relaxed for 100,000 MD steps under constant pressure and temperature. Then, the sample cooled down to 1475 K at ambient pressure with the cooling rate of about 10^{12} K/s. Next, the system relaxed using isothermal-isobaric (NPT) ensemble (in the isothermal-isobaric ensemble, moles (N), pressure (P) and temperature (T) conserved) to reach equilibrium state for 10^5 MD steps. Next, we keep the same temperature and compress at different pressures from 0–100 GPa. Finally, these models relaxed for a long time to reach the equilibrium at constant temperature and pressure for 10^6 MD steps and the system reaches steady state with the lowest energy. Finally, we obtained eight models for SiO_2 amorphous. The structural properties of each model calculated by averaging over one thousand configurations during the last 10^6 MD steps and compared with experimental data. To clarify the structural phase transitions, the structural characteristics and network structures calculated, analyzed, and visualized in detail [11].

3 Results and Discussion

Figure 1 shows the pair radial distribution functions (PRDF) $g_{Si–Si}(r)$, $g_{Si-O}(r)$ and $g_{O-O}(r)$ of glass SiO_2 at a temperature of 1475 K in the 0–100 GPa range. It also shows that there is a structural phase transition from amorphous to crystalline under compression. Specifically, at pressures below 30 GPa, the structure of the model is amorphous, at pressures beyond 30 GPa, the system has a crystalline structure. At 0 GPa, the first peak of PRDF of Si–Si, Si–O, O–O pairs locates at 3.10, 1.60 and 2.60 Å, respectively. These values are in good agreement with the experimental data [19–21]. It can be seen that the first peak position of the gSi-O(r) and gO-O (r) changes significantly with the pressure (Fig. 2). When increasing the pressure from 0–30 GPa, the Si–O distance increases gradually from 1.60–1.70 Å. In the 30 to 100 GPa range, the Si–O bond distance tends to decrease from 1.70 to 1.64 Å, respectively. Meanwhile, O–O pair bond distance decreases from 2.60 down to 2.38 Å with increasing pressure from 0 to 100 GPa, respectively. This reveals that under pressure, the O atoms tend to more densely arranged [14].

The Si–Si bond distance under compression showed in the pair radial distribution function $g_{Si-Si(r)}$ (see Fig. 1). The first peak position of the $g_{Si-Si(r)}$ function hardly changes in the pressure range from 0–30 GPa but it decreases at above 30 GPa. The change in shape of the $g_{Si-Si(r)}$ function with pressure showed subpeak starting at 10 GPa. The subpeak height increases with increasing pressure and becomes sharp

Fig. 1 The PRDF of SiO_2 glass at 1475 K under compression

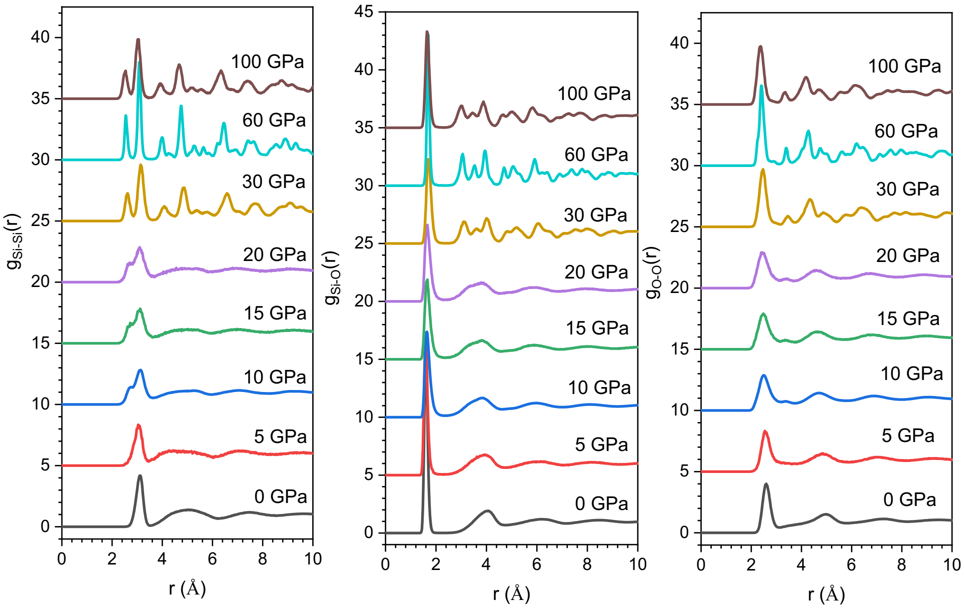

Fig. 2 The first peak of gSi-O (r) and gO-O (r) at 1475 K under compression

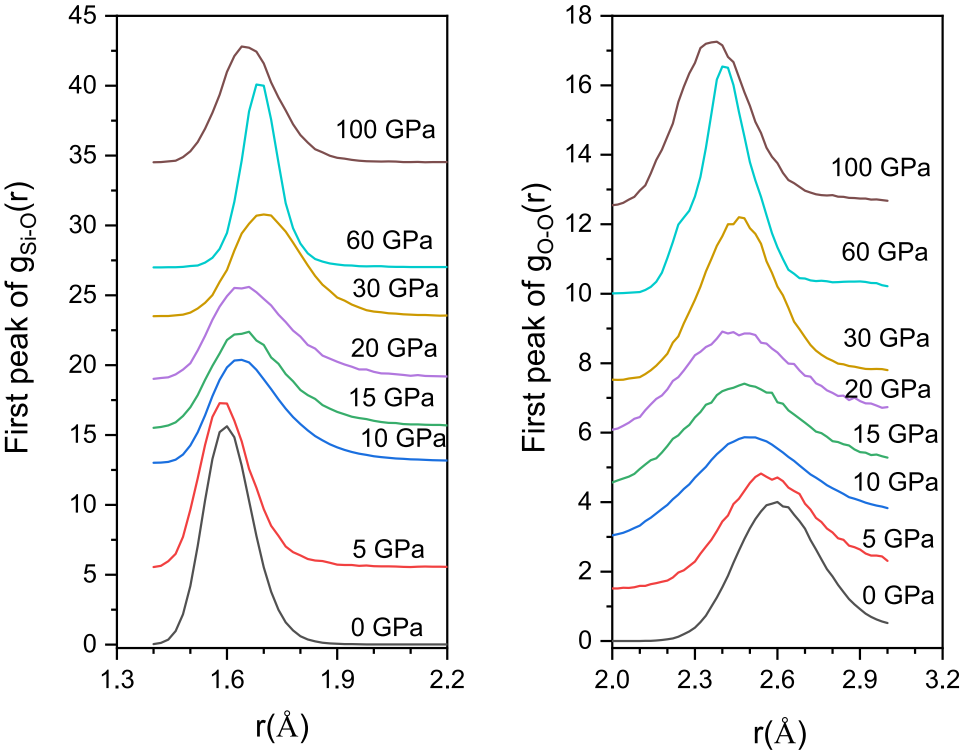

at 30 GPa. At this pressure, the position of the sub-peak locates at 2.62 Å and the first peak position is 3.14 Å. It shows the first peak position is larger than 3.06 Å that found in [11]. The structural state of SiO_2 at ambient pressure can be divided into 3 main states with temperature: glass (300-1400 K), glass transition (range 1475-1900 K) and liquid (above 1980 K). Experiments of Inamura et al. [22] have shown that the SiO_2 glass transitions to stishovite crystalline phase at a temperature of approximately 600 K when compressed under a pressure of 19.2 GPa, and when the temperature increased to 900 K the pressure is 11.9 GPa. This proves that SiO_2 is in the glass state, the higher the temperature, the lower the pressure of the stishovite crystal phase transition. In the study of F. S. El'kin et al. [23] also reported that the crystallization temperature of SiO_2 in glass state (below 730 K) with increasing pressure. Our simulation results at 500 K also show that the stishovite crystal phase transition pressure at 20 GPa is in perfect agreement with the experiment [22]. Ivan Saika-Voivod et al. shown that liquid SiO_2 (3000 K) is crystallized completely (Si has coordinate 6) at 44 GPa [24]. However, the phase transition of SiO_2 from amorphous to crystalline at the glass transition temperature range (1475 K-1900 K) has not studied yet. By molecular dynamics simulation method, we found that the stishovite crystal phase transition pressure at 1475 K is 30GPa. This result shows that the pressure–temperature dependence in the glass transition temperature region is completely different from the temperature range below 1400 K. This can explain as follows: At glass state, under compressive pressure, the atoms are more tightly packed, the bond length is shorter, the free volume region is narrower so that the model structure becomes stiff and crispy. In the glass transition temperature model, the thermal fluctuations of the atoms increase, the bond length close to the Si–Si pair bond distance of the model at room temperature and boundary pressure ($r_{Si-Si} = 3.12$ Å [21]). Viscosity of SiO_2 at near the transition temperature is higher at the low temperature. Therefore, glass transition models will need stronger compression to break the bond. We also predict that in the glass transition temperature region, the higher the temperature, the higher the crystal phase transition pressure. It may be necessary to investigate further for crystal phase transitions under pressure at temperature range 1475–1900 K to clarify this prediction.

Figure 3 also shows the difference in the glass transition pressure threshold of the low (at 500 K) and high (at 1475 K) temperature systems are 20 and 30 GPa, respectively. To clarify the structural phase transition, we conducted a survey of the coordination number distribution of the system.

Figure 4 shows the distribution of SiOx (x = 4,5,6) and OSiy (y = 2,3) coordination units at 1475 K (solid line). It shows that at low pressure, most of SiO_x basic units are SiO_4 and OSi_2. At ambient pressure, the fraction of SiO_4 and OSi_2 are all 99%. As pressure increases to 10 GPa, the fraction of SiO_4 units decreases quickly while the fraction of SiO_5 and SiO_6 units increase rapidly, and it shows quite

Fig. 3 The first peak of gSi-Si (r) under compression at 1475 K(**a**) and 500 K (**b**) in [11]

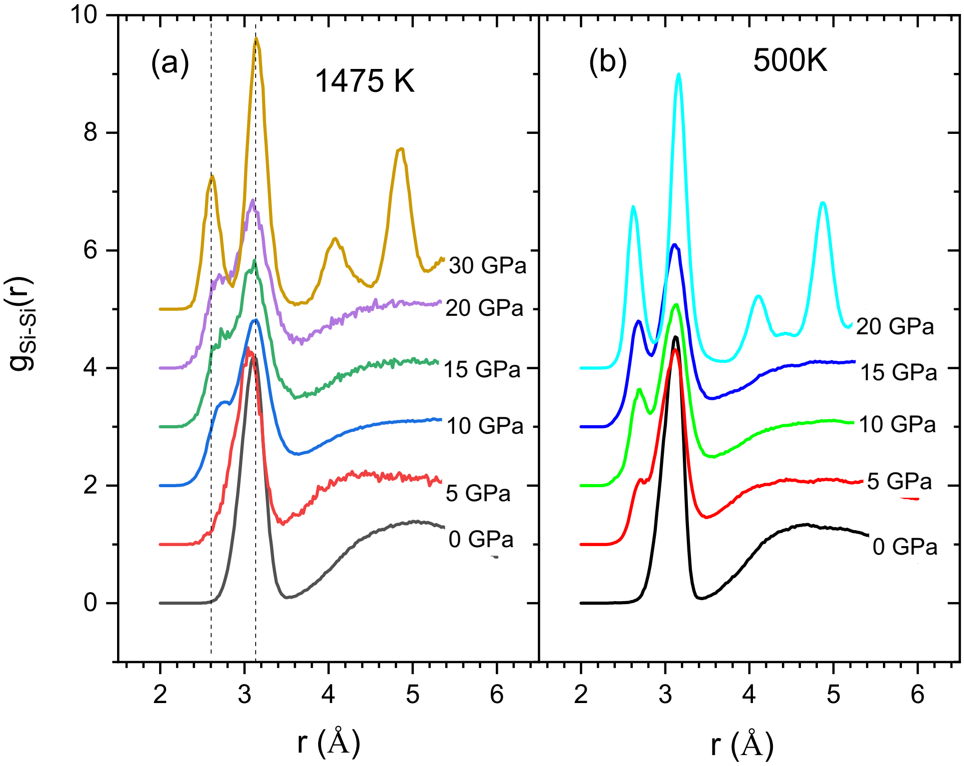

Fig. 4 The distribution of basic units SiOx (x = 4,5,6) (left) and OSiy (y = 2,3) (right) at 1475 K(solid lines) and 500 K (dashed lines [11]) under compression

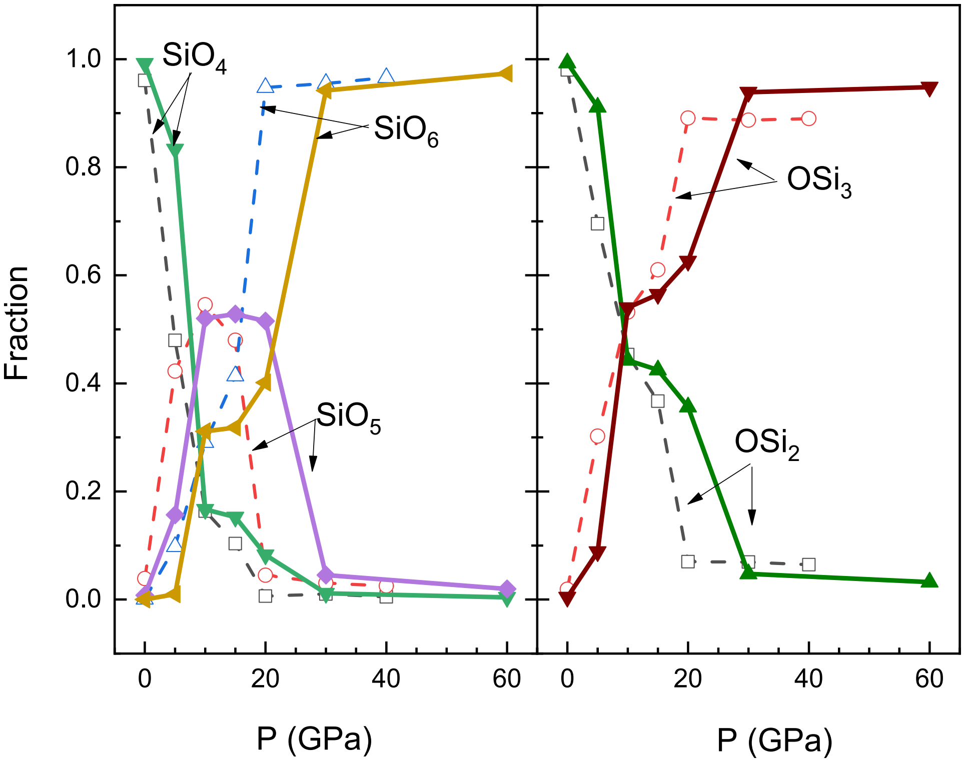

stability in the pressure range 10–20 GPa. Next, the fraction of SiO_5 units drops suddenly to only few percent while the fraction of SiO_6 increases rapidly to 97% in about 20–30 GPa. Structural phase transitions also indicated in the fraction of basic structural units OSiy. This is the change of coordinate number of O with compression pressure. In the pressure range from 0–10 GPa, the fraction of OSi_2 units decreased from 99 to 44%, while the fraction of OSi_3 units increased from 0.44% to 54%. In the pressure range of 10–20 GPa, the fraction of these units changes slowly by only few percent. As the pressure increases from 20 to 30 GPa, they change strongly. Specifically, the fraction of OSi_2 units decreases from 36% at 20aGPa pressure to 3% at 30 GPa while the fraction of OSi_3 units increases from 63 to 95%. We call the structure in the range of 10–20 GPa consisting of two types of basic structural units SiO_5 and SiO_6 as the intermediate structure. Thus, the phase transition from the tetrahedral structure to the intermediate structure is in the pressure range of 5–10 GPa, the intermediate state then maintains in the pressure range of 10–20 GPa with slight change in fraction of basic structural units. Increasing pressure from 20 to 30 GPa, the structural phase transition from the intermediate state to the octahedral structure takes place very strongly. The 30 GPa is the critical pressure value of the amorphous-crystalline phase transition. From the statistical survey of the distribution of basic structural units SiO_x and OSi_y via pressure at temperatures 1475 K and 500 K [11] (dashed line in Fig. 4), we show the difference in the phase transition process of the system. The distribution of coordination units of the 500 K sample is steeper, and the SiO_5 curve width is narrower than that of the 1475 K sample. This indicates that the fraction of SiO_4, SiO_5 and SiO_6 basic structural units in the 500 K system is sensitive to compression pressure [11, 14]. The amorphous-crystalline phase transition in the model 500 K happen at critical pressure of 20 GPa. The change in the proportion of the basic structural units caused by the change of the bond angle and the distance in each coordination unit and between the basic structural units. As we have known, the works [11, 14, 25] also show that the Si–O bond distance and O-Si–O bond angle in the SiO_4 and SiO_5 coordination units do not change with pressure. The main variation in SiO_6 units is the Si–O distance at high pressures from 30–100 GPa (see Fig. 5) and the Si–O-Si bond angle between two neighboring structural units (Fig. 6).

Figure 5 explains clearly why there is a change in the first peak position in the $g_{Si\text{-}O(r)}$ function with pressure (see Fig. 2). The Si–O bond distances in SiO_6 receive values of 1.72, 1.70 and 1.64 Å at pressure ranges of 0–30, 60 and 100 GPa, respectively. While the Si–O distances in SiO4 and SiO_5 have values of 1.62 and 1.66 Å, respectively. The increase of the Si–O distance is due to the increase of the high coordination number in the intermediate state.

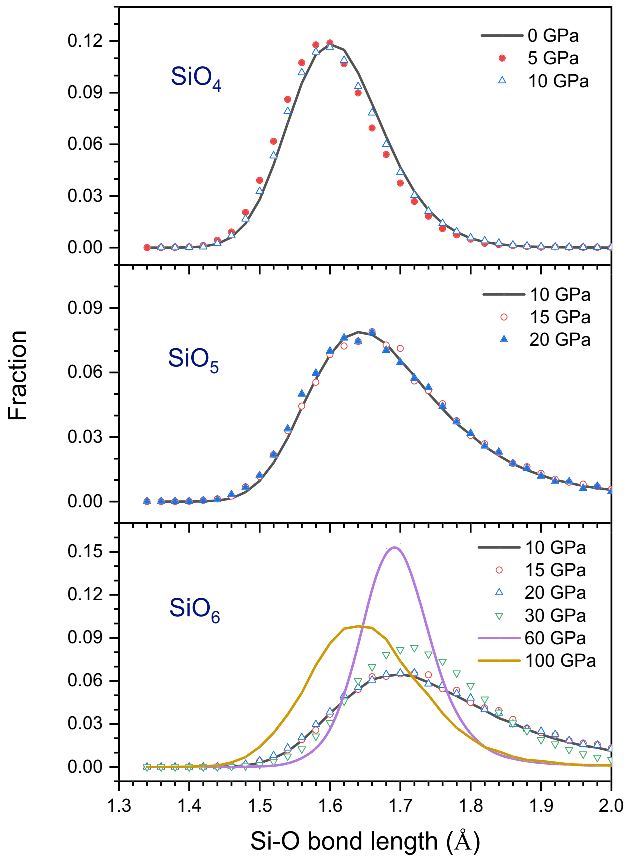

Fig. 5 The Si–O bond length distribution in SiOx (x = 4,5,6) under compression and temperature 1475 K

Figure 6 shows that the Si–O-Si bond angle decreases with pressure and increases the coordinate number of O from 2 to 3. The Si–O-Si bond angle of two-coordinated oxygen decreased from 150^0 to 140^0 with increasing pressure from 0–20 GPa [11, 26]. Fraction of three-coordinated O also increases in the range of 10–30 GPa. Thus, when compressing to 5 GPa, the tetrahedral structure of the system maintained and there is a slight change in the Si–O-Si bond angle [27]. This change leads to an increase of coordination number O atoms. The process of breaking bonds and rearranging atoms happens strongly when the model compressed to 10 GPa. In the range 10–20 GPa, the system exists as an intermediate state when it is little affected by compressive pressure. When the compressive pressure reaches a sufficiently high value of about 20–30 GPa, the considerable number of bonds broken and rearranged by atoms in a higher order degree. To clarify the bond distribution, we quantitatively calculate the vertex-, edge-, and face-shared links between neighboring structural units in the system. The calculation results shown in Fig. 7.

The visual images of vertex-shared (0 GPa), vertex- and edge-shared (10 GPa), face-shared (20 GPa) links presented in Fig. 8. Solid lines indicate the vertex-, edge-, face-shared

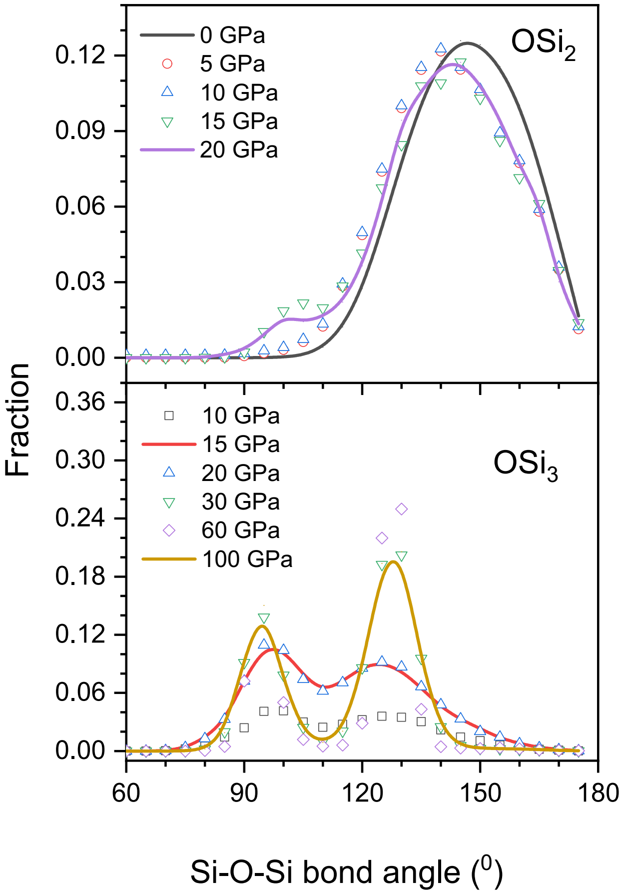

Fig. 6 The Si–O-Si bond angle distribution in OSiy (y = 2,3) under compression and temperature 1475 K

in this study, the dashed line is the result calculating in [11]. It shows that the basic structural units linked together by vertex- and edge-shared links.

The number of vertex- and edge-shared links increases rapidly with increasing pressure. The rate of increase described by the slope of the pressure dependent function and shows the strongest increase between 5–10 GPa and 20–30 GPa. In the 10–20 GP range, the number of these linkages change little, but the number of face-shared links is a maximum value, and they are 1.5 times higher than the number of face-shared links found in [11]. Face-shared links broken only when the compressive pressure is greater than 20 GPa. That is the cause of the sharp increase in the number of vertex- and edge-shared links in the pressure range of 20–30 GPa. From Fig. 4, it reveals that at pressures below 30 GPa, the number of vertex-, edge-, and face-shared links changes strongly with the pressure, while for the sample of 500 K it completes the structural phase transition at 20GPa. This is useful information to elucidate the predictions of phase transitions under pressure of the high temperature system given in reports [12, 17].

This again confirms that at high temperature, the increase in the number of face-shared links helps the intermediate state to be more stable with pressure. It causes a slower amorphous-crystalline phase transition because the face-shared links are more difficult to break than other link types. In report [25], it shown that SiO_2 has a tetrahedral structure at low pressure and an octahedral structure at high pressure. Structural phase transition is the change of the fraction of the basic structural units from SiO_4 to SiO_6 through the

Fig. 7 The average vertex-, edge- and face-shared link distribution on one Si atom under compression and temperature 1475 K (solid lines) and 500 K [11] (dashed line)

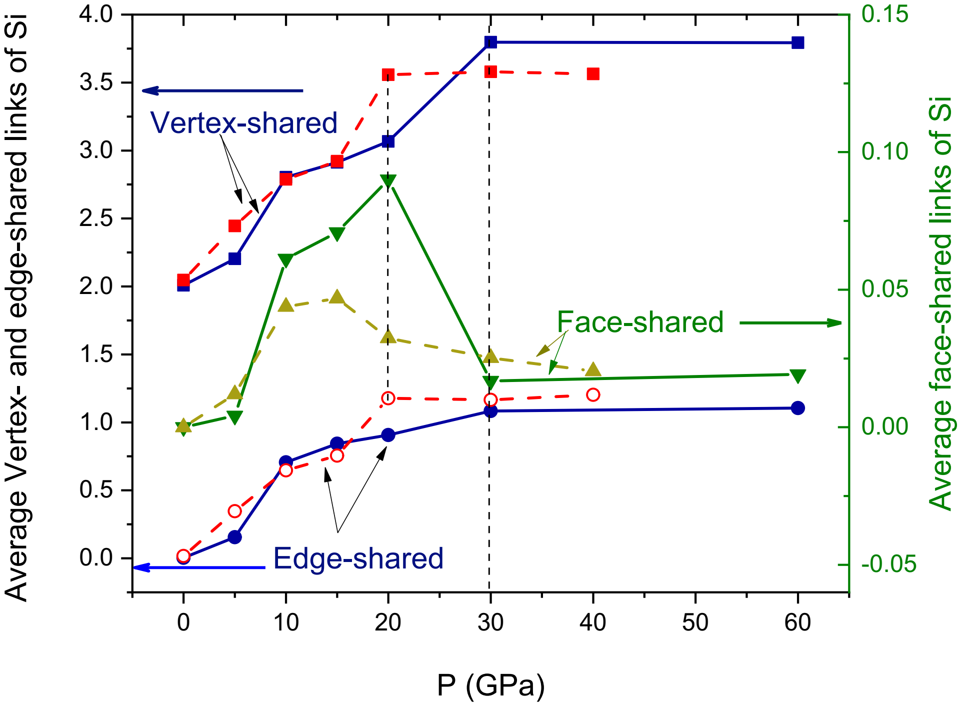

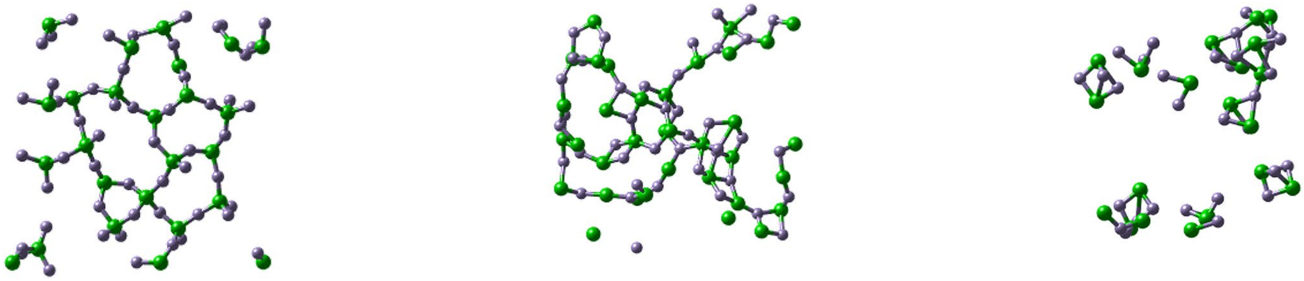

Fig. 8 The visual images of vertex-shared (left), vertex- and edge-shared (medium), face-shared (right) links

intermediate structural units SiO_5. Under the influence of compressive pressure, the fast or slow structural phase transition is completely dependent on the bond strength inside the basic structural units. Table 1 also shown that at the pressure range of 5–10 GPa, the tetrahedral structure is broken simultaneously and has a rearrangement of atoms to become a mixed structure consisting of two the main subnets are SiO_5 and SiO_6 clusters at 10 GPa.

Specifically, it also shows that the amorphous SiO_2 structure consists of the largest SiO_5 cluster containing 3469 atoms and the largest SiO_6 cluster containing 2498 atoms. There are a lot of small clusters SiO_4, SiO_5 and SiO_6 that besides the two largest clusters. There are small clusters of SiO_4 isolated and inserted with SiO5 clusters, so when compressed, it combines with SiO5 structural units to form SiO_6 through vertex- or edge-shared links. This statistically increases the number of vertex- and edge-shared links with the Si atom. Because of this, the number of face-shared links increases and maximum at 20 GPa. The increase in the Si–O distance leads to a decrease in the O–O distance, which causes the O atoms to increase in linking with the neighboring structural unit, so that the SiO_6 cluster expands while the SiO_4 and SiO_5 clusters shrunk. At above 20 GPa, there is a fast expansion of the largest cluster SiO_6. Now, the system has an octahedral structural network containing 99.4% atoms at 30 GPa. This result compared with data in [11, 27–29] and it reveals that at the glass transition temperature, the tetrahedral structure is quite stable under 5 GPa. The intermediate structure mostly affected by pressures in the 10–20 GPa range. The structural phase transition takes place strongly in two pressure ranges of 5–10 GPa and 20–30 GPa. This has influence with the phase transition at the low temperature model. At the glass transition temperature, the crystallization process under compression happens more slowly, the lifetime of the intermediate state is longer, and the bond strength is also stronger than that of the low temperature system.

4 Conclusion

The structural phase transition at glass transition temperature clarified through bond length, bond angle, coordination number distribution, links. The Si–Si bond distance is related to the phase transition pressure range of the investigated system.

The process of structural phase transition from amorphous to crystalline under compressive pressure depends on

Table 1 Distribution of the number of clusters and their size at different pressures at temperature 1475 K under compression. Nc and Na are the number of cluster and the number of atoms in one cluster, respectively

	0 GPa		5 GPa		10 GPa		15 GPa		20 GPa		30 GPa		60 GPa	
	Nc	Na	Nc	Na	Nc	Na	Nc	Na	Nc	Na	Nc	Na	Nc	Na
SiO4	**1**	**4983**	7	5–13	125	5	113	5	60	5	6	5	3	5
			1	**4322**	49	9–37	15	9–17	2	9				
SiO5	12	6–10	82	6–201	11	6–15	20	6–11	26	6	15	6	4	6
					1	**3469**	**1**	**3131**	12	10–33	4	11–15		
									1	**2740**				
SiO6			33	7–20	17	7	4	7	2	7	**1**	**4955**	**1**	**4978**
					10	11–25	**1**	**3443**	**1**	**3875**				
					1	**2498**								
SiO7					2	8	9	8	15	7–15	8	8–14	11	8–14

The number in bold indicates the number of atoms in a maximum cluster under pressure. For example, at a pressure of 5 GPa, the SiO_4 structural units connect together to form the largest cluster containing up to 4322 atoms. At 30 GPa the SiO_6 structural units connect together to form the largest cluster containing 4955 atoms. This is a demonstration of the phase transition from tetrahedral to octahedral structure under compression temperature. The intermediate structure consisting of two large clusters of SiO_5 and SiO_6 is quite stable in the pressure range 10–20 GPa because they have more face-shared links than the ones at low-temperature systems.

The critical pressure value for crystalline-amorphous phase transition is determined at 30 GPa for high-temperature (1475 K), and at 20 GPa for the low-temperature (500 K) model. The structural phase transition is related to the process of change in the number of vertex-, edge-, and face-shared links as well as the change in coordination number under the compression.

Author Contributions Nguyen Thu Nhan: constructed models, analyzed, summarized, and written reports. Nguyen Van Hong: constructed models. Mai Thi Lan: analyzed and processed the data. All authors have read and agreed to the published version of the manuscript.

Data Availability The data that support the findings of this study are available from the corresponding author upon reasonable request.

Declarations

Ethics Approval Not applicable.

Consent to Participate All authors have agreed to participate.

Informed Consent Statement Not applicable.

Consent for Publication All authors have agreed for publication.

Institutional Review Board Statement Not applicable.

Conflicts of Interest The authors declare that they have no conflict of interest.

Competing Interests The authors declare no competing interests.

References

1. Du T, Søren S, Theany T, Morten MS (2022) Oxide glasses under pressure: Recent insights from experiments and simulations. J Appl Phys 131:170901
2. Zarzycki J (1982) Glasses and the Vitreous State. Cambridge University Press, Cambridge, UK
3. Varshneya AK (2006) Fundamentals of Inorganic Glasses. Society of Glass Technology, Sheffield, UK
4. Dyre JC (2006) Colloquium: The glass transition and elastic models of glass-forming liquids. Rev Mod Phys 78:953–972
5. Kurkjian CR, Krol DM, Devine RB, Duraud JP, Dooryheé E (2000) Structure and Imperfections in Amorphous and Crystalline Silicon Dioxide. John Wiley and Sons, New York, 449
6. Klinger MI (2013) Glassy Disordered Systems: Glass Formation and Universal Anomalous Low-Energy Properties. World Scientific, London, UK
7. Sanditov DS, Ojovan MI, Darmaev MV (2020) Glass transition criterion and plastic deformation of glass. Physica B 582:411914
8. Tanaka H (2005) Two-order-parameter model of the liquid–glass transition. I. Relation between glass transition and crystallization. J Non-Cryst Solids 351:3371–3384
9. Nhan NT, Hung PK, Nghiep DM, Kim HS (2008) Molecular Dynamics Investigation on Microstructure and Void in Amorphous SiO2. Mater Trans 49:1212–1218
10. Vinh LT, Hung PK, Hong NV, Tu TT (2009) Local microstructure of silica glass. J Non-Cryst Solids 355:1215–1220
11. Nhan NT, Trang GTT, Iitaka T, Hong NV (2019) Crystallization of amorphous silica under compression. Can J Phys 97:1133–1139
12. Onodera et al (2020) Structure and properties of densified silica glass: characterizing the order within disorder. NPG Asia Mater 12:85
13. Preschera C, Vitali BP, Stefanski J, Jahn S, Lawrie BS, Wang Y (2017) Beyond sixfold coordinated Si in SiO2 glass at ultrahigh pressures. PNAS 114:10041–10046
14. Hong NV, Lan MT, Nhan NT, Hung PK (2013) Polyamorphism and origin of spatially heterogeneous dynamics in network-forming liquids under compression: Insight from visualization of molecular dynamics data. Appl Phys Lett 102:191908
15. Zeidler A, Salmon PS, Skinner LB (2014) Packing and the structural transformations in liquid and amorphous oxides from ambient to extreme conditions. Proc Natl Acad Sci 111:10045–10048
16. Salmon PS, Huang L (2017) Impact of pressure on the structure of glass and its material properties. MRS Bull 42:734–737
17. Ojovan MI, Tournier RF (2021) On Structural Rearrangements Near the Glass Transition Temperature in Amorphous Silica. Materials 14:5235
18. Van Beest BWH, Kramer GJ, van Santen RA (1990) Force fields for silicas and aluminophosphates based onab initiocalculations. Phys Rev Lett 64:1955–1958
19. Biswas RK, Khan P, Mukherjee S, Mukhopadhyay AK, Ghosh J, Muraleedharan K (2018) Study of short-range structure of amorphous Silica from PDF using Ag radiation in laboratory XRD system, RAMAN and NEXAFS. J Non-Cryst Solids 488:1–9
20. Vollmayr K, Kob W, Binder K (1996) Cooling-rate effects in amorphous silica: A computer-simulation study. Phys Rev B 54:15808–15827
21. Mozzi RL, Warren BE (1969) The structure of vitreous silica. J Appl Cryst 2:164–172
22. Inamura Y, Katayama Y, Utsumi W, Funakoshi K (2004) Transformations in the Intermediate-Range Structure of SiO_2 Glass under High Pressure and Temperature. Phys Rev Let 93:015501
23. El'kin FS, Brazhkin VV, Khvostantsev LG, Tsiok OB, Lyapin AG (2002) In situ Study of the Mechanism of Formation of Pressure-Densified SiO2 Glasses. JETP Lett 75:342–347
24. Saika-Voivod I, Poole PH, Bowles RK (2006) Test of classical nucleation theory on deeply supercooled high-pressure simulated silica. J Chem Phys 124:224709
25. Hung PK, Nhan NT (2010) Polyamorphism in the silica glass. Scr Mater 63:12–15
26. Mauri F et al (2000) Si-O-Si bond-angle distribution in vitreous silica from first principles 29Si NMR analysis. Phys Rev B 62:4786–4789
27. Ivan S, Francesco S, Tor G, Peter HP (2004) Phase diagram of silica from computer simulation. Phys Rev E 70:061507
28. Sato T, Funamori N (2008) Sixfold-coordinated amorphous polymorph of SiO2 under high pressure. Phys Rev Lett 101:255502
29. Petitgirard S et al (2019) Magma properties at deep Earth's conditions from electronic structure of silica. Geochem Persp Let 9:32–37